AD-A071 372 CALIFORNIA INST OF TECH PASADENA SEISMOLOGICAL LAB F/G 19/4
SHOCK EFFECTS IN CARBONATE MINERALS AND ROCKS.(U)
JUN 78 J VIZGIRDA, T J AHRENS DNA001-76-C-0218

UNCLASSIFIED DNA-4645F NL

| OF |
AD
A071372

END
DATE
FILMED
8-79
DDC

(12) LEVEL III

AD-E300 533

DNA 4645F

SHOCK EFFECTS IN CARBONATE MINERALS AND ROCKS

Joana Vizgirda
Thomas J. Ahrens
California Institute of Technology
Seismological Laboratory
Division of Geological and Planetary Sciences
Pasadena, California 91125

30 June 1978

Final Report for Period 1 January 1978—30 June 1978

CONTRACT No. DNA 001-76-C-0218

APPROVED FOR PUBLIC RELEASE;
DISTRIBUTION UNLIMITED.

THIS WORK SPONSORED BY THE DEFENSE NUCLEAR AGENCY
UNDER RDT&E RMSS CODE B344077464 Y99QAXSB04915 H2590D.

Prepared for

Director
DEFENSE NUCLEAR AGENCY
Washington, D. C. 20305

REPORT DOCUMENTATION PAGE

READ INSTRUCTIONS BEFORE COMPLETING FORM

1. REPORT NUMBER: DNA 4645F	2. GOVT ACCESSION NO. / 3. RECIPIENT'S CATALOG NUMBER
4. TITLE (and Subtitle): SHOCK EFFECTS IN CARBONATE MINERALS AND ROCKS	5. TYPE OF REPORT & PERIOD COVERED: Final Report for Period 1 Jan 78—30 Jun 78
	6. PERFORMING ORG. REPORT NUMBER
7. AUTHOR(s): Joana Vizgirda, Thomas J. Ahrens	8. CONTRACT OR GRANT NUMBER(s): DNA 001-76-C-0218
9. PERFORMING ORGANIZATION NAME AND ADDRESS: California Institute of Technology, Seismological Laboratory, Division of Geological and Planetary Sciences, Pasadena, California 91125	10. PROGRAM ELEMENT, PROJECT, TASK AREA & WORK UNIT NUMBERS: Subtask Y99QAXSB049-15
11. CONTROLLING OFFICE NAME AND ADDRESS: Director, Defense Nuclear Agency, Washington, D.C. 20305	12. REPORT DATE: 30 June 1978
	13. NUMBER OF PAGES: 24
14. MONITORING AGENCY NAME & ADDRESS (if different from Controlling Office)	15. SECURITY CLASS (of this report): UNCLASSIFIED
	15a. DECLASSIFICATION DOWNGRADING SCHEDULE

16. DISTRIBUTION STATEMENT (of this Report)

Approved for public release; distribution unlimited.

17. DISTRIBUTION STATEMENT (of the abstract entered in Block 20, if different from Report)

18. SUPPLEMENTARY NOTES

This work sponsored by the Defense Nuclear Agency under RDT&E RMSS Code B344077464 Y99QAXSB04915 H2590D.

19. KEY WORDS (Continue on reverse side if necessary and identify by block number)

Eniwetok
Pacific Test Site
Shock Waves
Cratering
Peak Pressures

20. ABSTRACT (Continue on reverse side if necessary and identify by block number)

The ESR spectra of Mn^{++} in naturally and laboratory shocked calcite crystals and coral core samples were studied and variations in several spectral parameters were found to be correlative with shock pressure. The amount of splitting in the central transition hyperfine component peaks was observed to decrease in the upper levels of the Cactus Crater core and in core samples shocked in the laboratory to progressively higher pressures. A comparison of the splitting amplitude between the two types of samples allows pressure

20. ABSTRACT (Continued)

assignments to the Cactus core of 3.3 GPa at 8m. ± 5m. and 2.0 GPa at 13m. ± 5m. Unshocked coral core samples showed no splitting amplitude variation with depth. Results from coral subjected to a long duration pressure pulse in the Miser's Bluff TNT experiment are generally inconsistent. Laboratory shocked single crystal calcite showed similar decreases in hyperfine peak splitting but at pressure levels three times greater than those producing comparable coral sample spectra. The decrease in peak splitting is interpreted to reflect small increases in cation-anion distances produced by mechanical energy input during the shock process. Another parameter, the non-central to central transition peak amplitude, is observed to decrease with increasing pressure in spectra of single crystal calcite, and may provide a means of empirically correlating very low ($<$4.5 GPa) shock pressure levels in calcite.

TABLE OF CONTENTS

	Page
INTRODUCTION	3
EXPERIMENTAL	3
RESULTS	4
Eniwetok Core Carbonates	4
Miser's Bluff Samples	10
DISCUSSION	15
REFERENCES	17

INTRODUCTION

Our investigations over the last six months have concentrated almost exclusively on the re-examination and refinement of the electron spin resonance technique as a means of detecting and placing quantitative pressure limits on shocked carbonate materials.

An extensive series of analyses on naturally and laboratory shocked and on unshocked samples of both single crystal calcite and mixed phase (calcite plus aragonite) coralline materials have verified some of our previously reported results (Vizgirda and Ahrens, 1977). Specifically, several spectral features, related to the amount of crystal field splitting in divalent manganese, a common trace element in calcite, show consistent variations with shock pressure.

Previously reported variations in the amplitude of the radiation damage center peaks are no longer believed to be caused by shock induced annealing. Control samples from an unshocked core (XRU-3) produced a radiation damage center amplitude trend similar to that observed in the Cactus Crater core (below the contaminated uppermost levels), i.e., a slight increase in the deeper core levels. Consequently, it is concluded that the observed amplitude increase with depth is caused by greater numbers of defects (hole centers and electron centers) produced by radiation from elements such as ^{40}K, ^{238}U and ^{232}Th, and, hence, merely represents the increasing age of the deeper core rock. (A similar age variation has been observed in a stalacite by M. Ikeya, 1975.) A low pressure shock history does not appear capable of modifying this figure to any great extent.

EXPERIMENTAL

All spectra were recorded at X-band frequencies (9.1 → 9.5 GHZ) on a Varian V-4500 spectrometer.* Room temperature second derivative spectra were recorded at modulation amplitudes ranging from 5 to 0.63 gauss to investigate

---

*The spectrometer used in this study is a facility of the Noyes Laboratory, CIT. Previous spectra were recorded by F. Tsay at the Jet Propulsion Lab. In comparing the two sets of data, allowance must be made for the instrumental difference.

the dependancy of crystal field splitting on this parameter. Peak splitting remained constant at low modulation levels (0.63G → 1.6G) and increased at higher amplitudes; a modulation amplitude of 1 gauss provided an optimum signal to noise ratio in most cases and 90% of the measured spectra were recorded at this setting.

Most samples of Eniwetok core limestone were hand friable or easily fractured and could be directly placed into 4mm diameter ESR quartz tubes. Several samples required grinding with mortar and pestle, but there was no correlation between the amount of grinding needed and the crystal field splitting amplitude. The single crystal calcite samples readily fractured and required minimum handling.

RESULTS

Eniwetok Core Carbonates

All 16 samples of Cactus Crater core were re-analyzed using the CIT spectrometer. Values of the hyperfine component peak splittings were consistently 5 gauss lower than previously recorded values; however, the trend of reduced splitting values in upper core level samples is verified upon re-examination. For three of the samples, several aliquots were prepared and the spectra measured; in all cases, splitting values for the various aliquots of the same sample agreed to within less than 0.5 gauss. From the topmost Cactus sample (8.1 meters), a fine pebble conglomerate, aliquots of both the very fine grained matrix material and the clasts were analyzed; the clasts (coral fragments) showed no resolveable Mn^{++} signal, and the reported spectrum for this sample is of the matrix material.

Consistent variations in spectral features from the top to the bottom of the core can be observed in Fig. 1. (The spectra were taken at a uniform 1 gauss modulation amplitude, therefore line shapes can be directly compared.) The lowest field Mn^{++} hyperfine component (the left-hand arrow in the figure) is observed as a single peak in the 8.1, 11.8 and 12.2 meter samples; below this depth it is clearly split into two sub-peaks and this splitting is increasingly well-defined in lower core samples. The highest field hyperfine component (right-hand arrow in figure) remains split throughout the extent of the core, but the amplitude of the splitting decreases approximately 30% from the bottom to the top. In addition, the highest field hyperfine peak displays

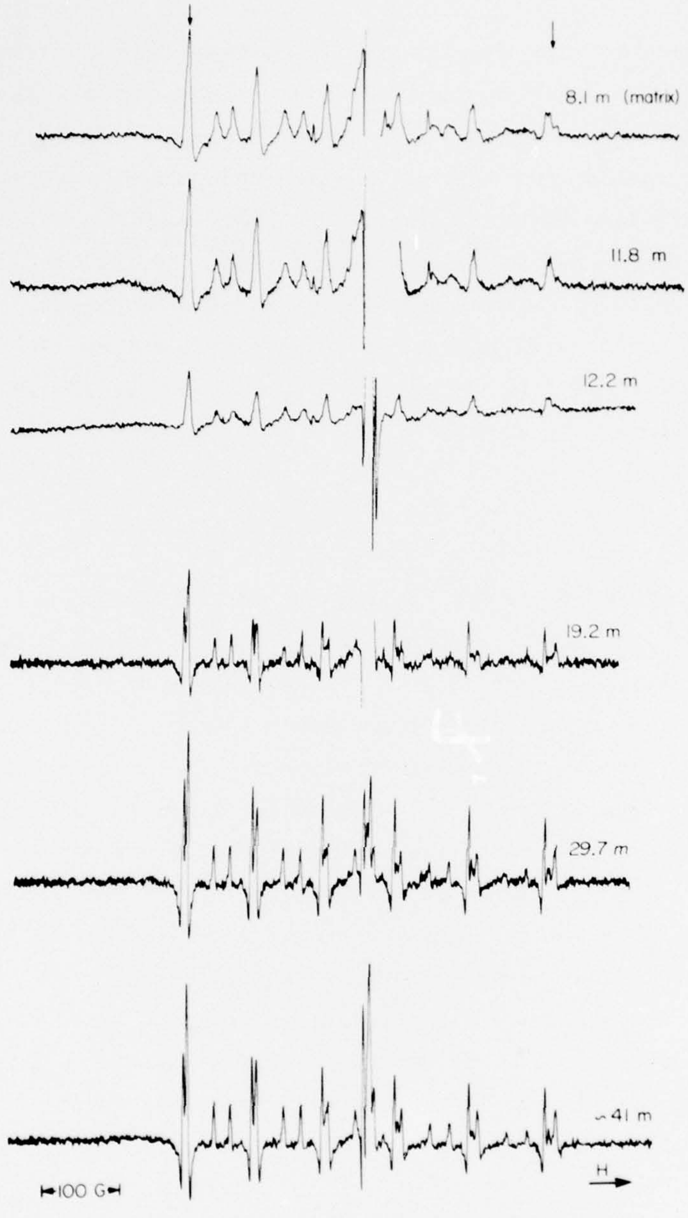

Figure 1. Second derivative ESR spectra of Mn^{++} in Cactus Crater core (XC-1) samples from several depths. Note the consistent variation with depth in the splitting amplitude of the central transition hyperfine component peaks, particularly the highest and lowest field peaks (indicated with arrows). Magnetic field strength increases toward the right.

a more complex substructure; the lower field "sub-peak" of this component is observed to be further split in the three upper core samples. The amplitude of this splitting is 4.5 ± 0.5 gauss in the 8.1 and 11.8 meter and 3 ± 0.5 gauss in the 12.2 meter samples; no such small scale splitting is observed in other XC-1 samples. Splitting (large scale) is, in fact, observed in all 6 hyperfine peaks in samples taken from below 12.2 meters. For the 12.2 m sample, however, splitting can be resolved for only the 3 upper field components. The highest field hyperfine peak shows splitting for all samples; the amount of this splitting has been measured and the results are plotted in Fig. 2. The equation for the power curve fit for the XC-1 data is:

$$HPS = 8.07d^{0.16} \tag{1}$$

where HPS is the highest field Mn^{++} hyperfine peak splitting, measured in gauss, and d is core depth in meters; the correlation coefficient, r^2, is 0.85.

Coral core samples shock-loaded in the laboratory at pressures up to 3.3 GPa have also been re-examined; resolveable spectra have been obtained for only three samples and these are reproduced in Fig. 3. Note the similarity in the spectra of the 2.0 GPa laboratory shocked coral and the XC-1 12.2 meter sample; in both cases, *only the three high field hyperfine peaks are* resolveably split, and the measured amplitude of splitting of the highest field component is 12 ± 0.5 gauss. The two sub-peaks of the highest field component are somewhat difficult to isolate in the 3.3 GPa shocked sample spectrum, but slightly higher modulation traces give a reading of 11 ± 2 gauss. Results from these experimentally shocked samples are superimposed on the power curve fit to XC-1 data in Fig. 2. Uncertainties in assignment of pressure levels to certain depths were determined by calculating the standard deviation of the XC-1 data residuals.

Eight samples from the XRU-3 core were analyzed and measurements made on the splitting in the highest field hyperfine component. The results are plotted in Fig. 4. No trend is observed in the data; in particular, the upper core levels do not show any decrease in the amount of splitting. A least squares fit line to the data provides the relationship:

$$HPS = -0.008d + 14.42 \tag{2}$$

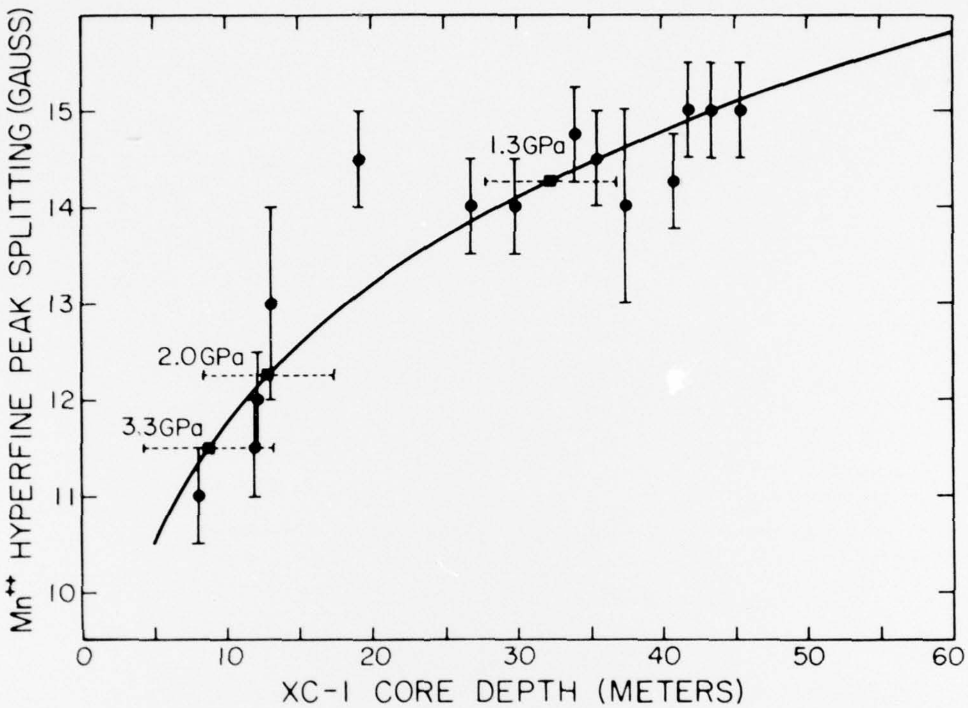

Figure 2. Variation of Mn^{++} hyperfine peak splitting, as measured for the highest field component, with depth in the Cactus Crater core. Circles represent the Cactus data. Squares represent laboratory shocked coral core samples; the numbers above the squares are shock pressures in gigapascals.

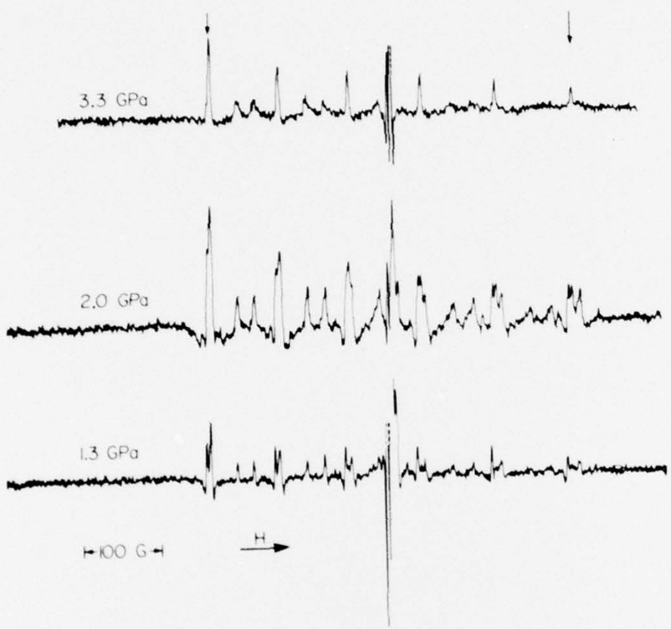

Figure 3. Coral core (XRU-3) samples experimentally shocked to indicated pressures (in GPa). Note the variation with pressure in the splitting of the central transition hyperfine component peaks.

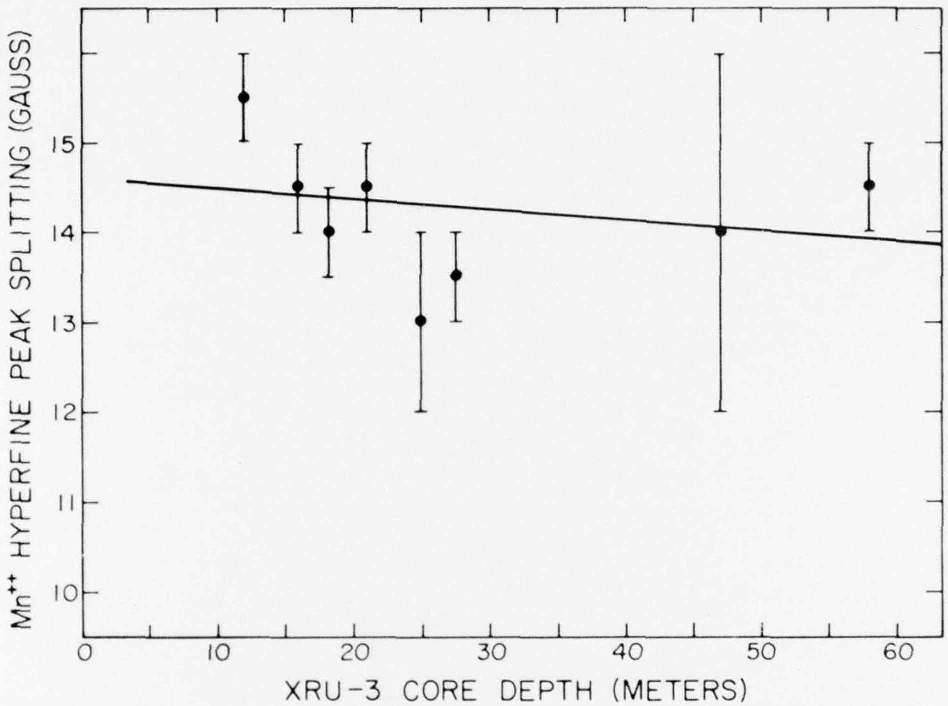

Figure 4. Highest field Mn^{++} hyperfine peak splitting variation with depth in the unshocked XRU-3 core.

The XRU-3 data (together with the experimentally shocked samples) substantiates the observed splitting variation in the XC-1 core as a shock deformation feature and not a reflection of trends in lithology, cementation, compaction, etc.

Miser's Bluff Samples

ESR spectra of twelve samples, 6 calcite and 6 coral, shocked in the Miser's Bluff TNT blast of December 1977 were obtained and measured. Six cylindrical sample assemblies were emplaced in two different holes in alluvium. As discussed below these appear to not have been dynamically loaded in a very uniform or monotonic manner. This is probably a consequence of inherent local inhomogeneities in the environment.

Results for the coral samples do not entirely agree with the calculated experimental pressures. On the basis of the onset and progression of splitting in the three lower field hyperfine components, the samples can be qualitatively ranked, in order of decreasing shock effect, as follows: cylinders #2, #3, #1, #4, #5 and #6. The calculated pressures for these cylinders (in that order) are .3, 0.03, 1.0, 0.5, 0.1 and 0.005 GPa. Hyperfine peak splitting amplitudes follow a bimodal distribution; samples from cylinders #2, #3 and #1 show a splitting of 11 to 12 gauss, while those from #4 and #6 show values of 15 and 14.5 respectively. The spectra for sample #5 shows very well defined peaks and generally resembles unshocked crystalline calcite spectra; the splitting amplitude of the highest field peak is 9.75 gauss. The anomalous absorption in this spectra may represent one orientation of a large single crystal of calcite dominating the average powder pattern. Thus except for sample #5, the two types of ESR criteria ("qualitative" and measured splitting) divide the samples into a definitely shock affected group consisting of cylinders #2, #3 and #1, and cylinders #4, #5 and #6 whose coral samples show little or no shock damage. Curiously, these two clusters correspond to the two holes in which the cylinders were emplaced. Direct comparison with laboratory data is possible in only one case; spectra from coral sample #3 resembles that of coral laboratory shocked to 2.0 GPa levels.

Measured hyperfine peak splitting values for the Iceland spar calcite samples shocked in the Miser's Bluff blast are all very similar and fall in the "unshocked range" of 14.25 to 15 gauss. In order to investigate other spectral features which may be sensitive to shock pressure levels lower than those necessary for annihilating splitting of hyperfine component peaks, unshocked and laboratory shocked calcite samples were analyzed. These features are labeled on a spectrum of unshocked Iceland spar in Fig. 5. The 6 most prominent peaks are the hyperfine components due to the central spin transition, $M_S = {}^{+}1/2 \leftrightarrow {}^{-}1/2$, $\Delta m_I = 0$. (It is variations in these features we have been considering up to now.) Absorption peaks due to non-central spin transitions are indicated on the high and low field ends of the spectrum. Another set of absorption lines in the central portion of the spectrum are those corresponding to forbidden transitions, $M_S = {}^{+}1/2 \leftrightarrow {}^{-}1/2$, $\Delta m_I = \pm 1$.

Four spectra of experimentally shocked single crystal calcite are reproduced in Fig. 6. Absorption peaks due to non-central transitions are indicated by arrows on the top spectra. The amplitude of these peaks has decreased significantly in the sample shocked to 3.5 GPa and has completely disappeared in the 5.5 GPa sample. Note also that, even in the highest shocked sample (6.5 GPa) splitting is evident in all 6 central transition hyperfine peaks.

Three of the Miser's Bluff shocked calcite spectra are shown in Fig. 7. All show clearly resolved splitting in the central transition hyperfine peaks. However, shock deformation is indicated by the reduced amplitude of the non-central transition peaks, particularly in the highest shocked sample (cylinder #1). Looking at the ratio of non-central to central transition peak amplitudes, the calcite samples can be grouped into those showing reduced ratios indicative of shock deformation, cylinders 1, 2 and 3, and those with approximately constant ratios comparable to unshocked Iceland spar, cylinders 4, 5 and 6. Clearly, the Miser's Bluff sample spectra all indicate shock deformation levels significantly less than 3.5 GPa; however, not enough samples experimentally shocked in the 0.5 → 2.0 GPa range are available to more precisely quantify deformation levels.

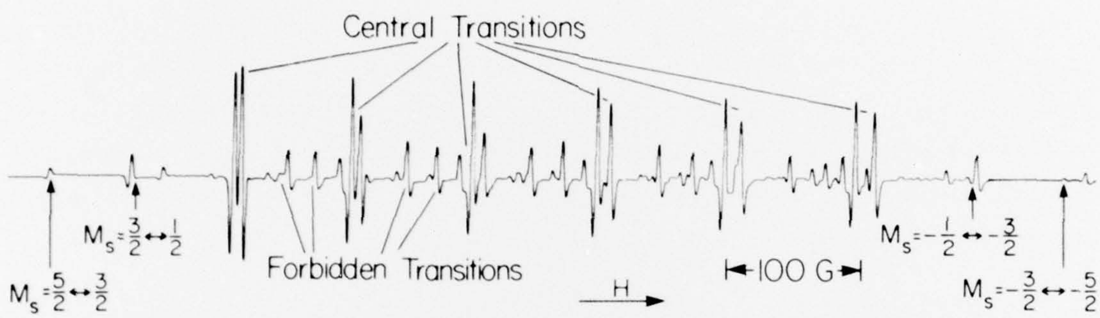

Figure 5. *Second derivative spectrum of* Mn^{++} *in a powder sample of* unshocked calcite (variety Iceland spar). The six prominent split peaks are the hyperfine components due to the central transitions, $M_S = {}^{+}1/2 \leftrightarrow {}^{-}1/2$, $\Delta m_I = 0$; the intervening lower intensity absorptions are due to forbidden transitions ($M_S = +1/2 \leftrightarrow {}^{-}1/2$, $\Delta m_I = \pm 1$). Hyperfine components corresponding to non-central transitions are observed at the high and low field ends of the spectrum.

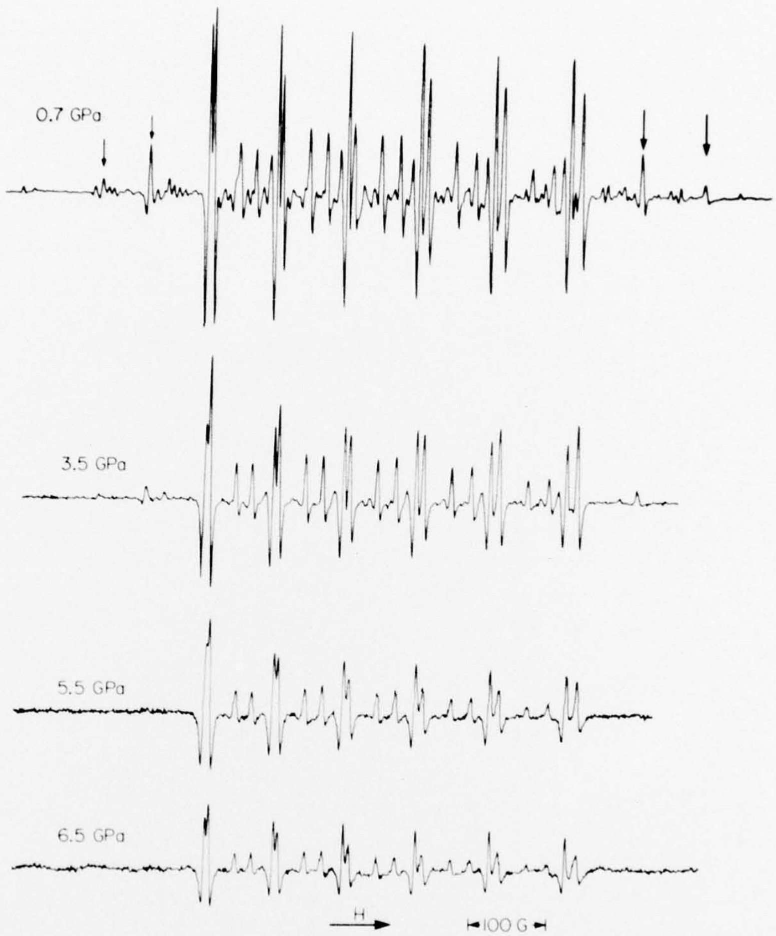

Figure 6. Second derivative ESR spectra of Mn^{++} in powder samples of experimentally shocked calcite, variety Iceland spar. Note the decreasing amplitude of the absorption peaks corresponding to the non-central transitions (indicated by arrows) with increasing shock pressure.

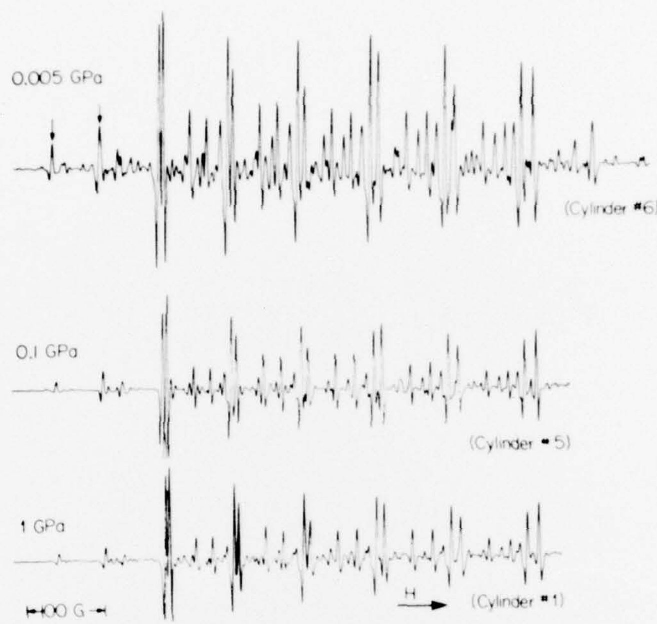

Figure 7. Iceland spar shock loaded in the Miser's Bluff TNT blast. Note the (slightly) decreasing amplitudes of the Mn^{++} non-central transition peaks (indicated by arrows) with increasing shock pressure.

DISCUSSION

In the discussion of both Eniwetok core and Miser's Bluff sample results, variations with shock pressure were observed in two spectral parameters, i.e., in the amount of splitting in the Mn^{++} central transition hyperfine component peaks, and in the non-central to central transition peak amplitude ratios.

The first of these features, the splitting amplitude is due to absorption at two extreme resonance positions, occurring at $\theta = 45^{o}$ (high field peak) and $\theta = 90^{o}$ (low field peak), for each hyperfine component. The transition energy term describing the amplitude of the separation (in gauss) is:

$$\Delta H = \frac{11\ D^2}{2g^2\beta^2 H} - \frac{75\ AD^2 m_I}{2g^3\beta^3 H^2} \qquad (3)$$

Where D (gauss) is the crystal field splitting parameter, A (gauss) is the hyperfine coupling constant, H (gauss) is the magnetic field corresponding to an unshifted resonance line, β is the Bohr magneton, g is the (isotropic) spectroscopic splitting factor, and m_I the nuclear spin of Mn^{++} (Tsay et al., 1977). Since the m_I dependent term in Eq. 3 will change sign in going from the low-field to the high-field side of the spectrum, the amount of splitting increases in the higher field hyperfine peaks. Our observations are consistent with theoretical variations; the decrease (and eventual disappearance) of splitting in the lowest field hyperfine peak is invariably linked to a similar decrease in the highest field peak.

According to electrostatic theory, the crystal field splitting parameter is approximately proportional to the inverse of the fifth power of the cation-anion distance (Orgel, 1957); this inverse relationship has been verified in an ESR investigation of forsterite (Rager, 1977). The following can thus be concluded from our observations of decreasing crystal field splitting parameters: recovery from increasing shock pressure has the effect of, on the average, increasing the cation-anion distance in the calcite lattice. This increase cannot at present be quantified, but is probably of the order of thousandths of angstroms. A similar increase in lattice parameter with shock deformation has been reported by Chao, 1968 in heavily shocked quartz from the Ries Crater in Germany, using X-ray techniques.

Thus, it is possible that what the ESR method is detecting in shocked carbonate samples is a very slight enlargement of the unit cell resulting from input of mechanical energy in the shock and rarefaction process.

The second observation, that is the decrease in non-central to central transition peak amplitudes with increasing pressure, is not readily understood on theoretical grounds, but has been observed by other workers (Gager et al., 1964).

A curious aspect encountered in investigation of the Miser's Bluff samples is the difference in results between the calcite and the mixed phase coral samples. The latter clearly showed a shock effect as measured by the decreased splitting of the highest field hyperfine peak. The calcite samples, on the other hand, showed a constant amount of splitting; however laboratory samples shocked to higher pressure levels than those in the Miser's Bluff blast did show a measureable decrease in this splitting. Thus, it appears that mixed phase carbonate materials are more readily deformed at a given stress level, by the shock process than single crystal calcite.

High precision level X-ray powder diffraction studies are being undertaken to see if there has been any change in the lattice parameters of the Miser's Bluff calcite and aragonite samples.

REFERENCES

Chao, E. C. T., Pressure and temperature histories of impact metamorphosed rocks - Based on petrographic observations. N. Jb. Miner. Abh., 108, No. 3, pp. 209-246 (1968).

Gager, W. B., Klein, M. J., and Jones, W. H., The generation of vacancies in MgO single crystals by explosive shock. Applied Physics Letters, 5, No. 7, pp. 131-132 (1964).

Ikeya, M., Dating a stalactite by electron paramagnetic resonance. Nature, 255, pp. 48-50 (1975).

Orgel, L. E., Ion compression and the colour of ruby. Nature, 179, p. 1348 (1957).

Rager, H., Electron spin resonance of trivalent chromium in forsterite, Mg_2SiO_4. Phys. Chem. Minerals, 1, pp. 371-378 (1977).

Tsay, F., Manatt, S. L., and Chan, S. I., Electron spin resonance of manganous ions in frozen methanol solution. Chemical Physics Letters, 17, No. 2, pp. 223-226 (1972).

Vizgirda, J. and Ahrens, T. J., Interim Final Report, (1977).

DISTRIBUTION LIST

DEPARTMENT OF DEFENSE

Assistant to the Secretary of Defense
ATTN: Executive Assistant

Defense Advanced Rsch. Proj. Agency
ATTN: TIO

Defense Civil Preparedness Agency
ATTN: Hazard Eva. & Vul. Red. Div., G. Sisson

Defense Documentation Center
12 cy ATTN: DD

Defense Intelligence Agency
ATTN: DB-4E
ATTN: DB-4C, E. O'Farrell

Defense Nuclear Agency
ATTN: DDST
4 cy ATTN: TITL
2 cy ATTN: SPSS

Field Command
Defense Nuclear Agency
ATTN: FCTMOF
ATTN: FCPR

Field Command
Defense Nuclear Agency
ATTN: FCPRL

Interservice Nuclear Weapons School
ATTN: TTV

NATO School (SHAPE)
ATTN: U.S. Documents Officer

Under Secy. of Def. for Rsch. & Engrg
ATTN: Strategic & Space Systems (OS)

WWMCCS System Engineering Org.
ATTN: T. Neighbors

DEPARTMENT OF THE ARMY

BMD Advanced Technology Center
Department of the Army
ATTN: 1CRDABH-X
ATTN: ATC-T

Chief of Engineers
Department of the Army
ATTN: DAEN-RDM
ATTN: DAEN-MCE-D

Harry Diamond Laboratories
Department of the Army
ATTN: DELHD-I-TL
ATTN: DELHD-N-P

U.S. Army Ballistic Research Labs.
ATTN: Technical Library
ATTN: DRDAR-PLE, J. Keefer

U.S. Army Engineer Center
ATTN: DT-LRC

DEPARTMENT OF THE ARMY (Continued)

U.S. Army Engineer Div. Huntsville
ATTN: HNDED-SR

U.S. Army Engineer Div. Ohio River
ATTN: ORDAS-L

U.S. Army Engr. Waterways Exper. Station
ATTN: Library
ATTN: G. Jackson
ATTN: J. Strange
ATTN: L. Ingram
ATTN: W. Flathau
ATTN: J. Drake

U.S. Army Material & Mechanics Rsch. Ctr.
ATTN: Technical Library

U.S. Army Materiel Dev. & Readiness Cmd.
ATTN: DRXAM-TL

U.S. Army Missile R&D Command
ATTN: RSIC

U.S. Army Nuclear & Chemical Agency
ATTN: Library

DEPARTMENT OF THE NAVY

Civil Engineering Laboratory
Naval Construction Battalion Center
ATTN: Code L08A
ATTN: R. Odello
ATTN: S. Takahashi

Naval Facilities Engineering Command
ATTN: Code 09M22C

Naval Material Command
ATTN: MAT 08T-22

Naval Postgraduate School
ATTN: Code 0142

Naval Research Laboratory
ATTN: Code 2627

Naval Surface Weapons Center
ATTN: Code F31

Naval Surface Weapons Center
ATTN: Tech. Library & Info. Services Branch

Naval War College
ATTN: Code E-11

Naval Weapons Evaluation Facility
ATTN: Code 10

Office of Naval Research
ATTN: Code 474, N. Perrone
ATTN: Code 715

Strategic Systems Project Office
Department of the Navy
ATTN: NSP-43

DEPARTMENT OF THE AIR FORCE

Air Force Geophysics Laboratory
ATTN: LWW, K. Thompson

Air Force Institute of Technology, Air University
ATTN: Library

Air Force Systems Command
ATTN: DLW

Air Force Weapons Laboratory
ATTN: DE, M. Plamondon
ATTN: SUL
ATTN: DES, J. Thomas
ATTN: DES, J. Shinn

Assistant Chief of Staff
Intelligence
Department of the Air Force
ATTN: INT

Deputy Chief of Staff
Research, Development & Acq.
Department of the Air Force
ATTN: AFRDQSM

Foreign Technology Division, AFSC
ATTN: NIIS Library

Rome Air Development Center, AFSC
ATTN: TSLD

Space & Missile Systems Organization
Air Force Systems Command
ATTN: MNN

Strategic Air Command
Department of the Air Force
ATTN: NRI-STINFO Library

Deputy Chief of Staff
Logistics & Engineering
Department of the Air Force
ATTN: LEEE

DEPARTMENT OF ENERGY

Department of Energy
ATTN: Technical Library

Department of Energy
ATTN: Classified Library

Department of Energy
ATTN: Technical Library

DEPARTMENT OF ENERGY CONTRACTORS

Lawrence Livermore Laboratory
ATTN: Technical Information Dept. Library
ATTN: L-96, L. Woodruff

Los Alamos Scientific Laboratory
ATTN: Reports Library
ATTN: R. Bridwell

Sandia Laboratories
ATTN: Library & Security Classification Div.

Sandia Laboratories
ATTN: A. Chabai
2 cy ATTN: 3141/L. Hill

OTHER GOVERNMENT AGENCIES

Central Intelligence Agency
ATTN: RD/SI, Rm. 5G48, Hq. Bldg. for J. Ingley

Department of the Interior
Bureau of Mines
ATTN: Technical Library

DEPARTMENT OF DEFENSE CONTRACTORS

Aerospace Corp.
ATTN: Technical Information Services

Agbabian Associates
ATTN: M. Agbabian

Applied Theory, Inc.
2 cy ATTN: J. Trulio

Avco Research & Systems Group
ATTN: Library A830

BDM Corp.
ATTN: Corporate Library

Boeing Co.
ATTN: Aerospace Library

California Institute of Technology
ATTN: J. Vizgirda
ATTN: T. Aherns

California Research & Technology, Inc.
ATTN: Library
ATTN: K. Kreyenhagen
ATTN: S. Shuster

California Research & Technology, Inc.
ATTN: D. Orphal

Calspan Corp.
ATTN: Library

Civil/Nuclear Systems Corp.
ATTN: J. Bratton

University of Dayton
Industrial Security Super KL-505
ATTN: H. Swift

University of Denver
Colorado Seminary
Denver Research Institute
ATTN: J. Wisotski

EG&G Washington Analytical Services Center, Inc.
ATTN: Library

Eric H. Wang
Civil Engineering Rsch. Fac.
ATTN: N. Baum

Gard, Inc.
ATTN: G. Neidhardt

General Electric Company-TEMPO
Center for Advanced Studies
ATTN: DASIAC

DEPARTMENT OF DEFENSE CONTRACTORS (Continued)

IIT Research Institute
ATTN: M. Johnson
ATTN: R. Welch
ATTN: Documents Library

University of Illinois
Consulting Services
ATTN: N. Newmark

Institute for Defense Analyses
ATTN: Classified Library

Kaman AviDyne
Division of Kaman Sciences Corp.
ATTN: E. Criscione
ATTN: N. Hobbs
ATTN: Library

Kaman Sciences Corp.
ATTN: Library

Lockheed Missiles and Space Co., Inc.
ATTN: T. Geers
ATTN: Technical Information Center D/Coll.

McDonnell Douglas Corp.
ATTN: R. Halprin

Merritt CASES, Inc.
ATTN: J. Merritt
ATTN: Library

Oak Ridge National Laboratory
Union Carbide Corporation
Nuclear Division
ATTN: Technical Library
ATTN: Civil Def. Res. Proj.

Physics International Co.
ATTN: J. Thomsen
ATTN: L. Behrmann
ATTN: Technical Library
ATTN: E. Moore
ATTN: F. Sauer

R & D Associates
ATTN: C. MacDonald
ATTN: R. Port
ATTN: Technical Information Center
ATTN: J. Lewis
ATTN: A. Latter

R & D Associates
ATTN: H. Cooper

Science Applications, Inc.
ATTN: Technical Library

DEPARTMENT OF DEFENSE CONTRACTORS (Continued)

Science Applications, Inc.
ATTN: D. Maxwell
ATTN: D. Bernstein

Southwest Research Institute
ATTN: W. Baker
ATTN: A. Wenzel

SRI International
ATTN: B. Gasten
ATTN: G. Abrahamson
ATTN: D. Keough
ATTN: Y. Gupta

Systems, Science & Software, Inc.
ATTN: Library
ATTN: D. Grine
ATTN: T. Cherry
ATTN: T. Riney

Systems, Science & Software, Inc.
ATTN: J. Murphy

Terra Tek, Inc.
ATTN: S. Green
ATTN: Library
ATTN: A. Abou-Sayed

Tetra Tech, Inc.
ATTN: Library

TRW Defense & Space Sys. Group
ATTN: Technical Information Center
ATTN: P. Bhutta
2 cy ATTN: P. Dai

TRW Defense & Space Sys. Group
ATTN: E. Wong

Vela Seismological Center
ATTN: G. Ullrich

Weidlinger Assoc., Consulting Engineers
ATTN: M. Baron
ATTN: I. Sandler

Weidlinger Assoc., Consulting Engineers
ATTN: J. Isenberg